ISBN: 978-3-95450-262-2 ISSN: 2673-5350 doi: 10.18429/JACoW-IBIC2025-TUBC02

BEAM DIAGNOSTICS, DATA ACQUISITION SYSTEM, AND APPLICATIONS OF MACHINE LEARNING AT THE KEK e-/e+ LINAC

F. Miyahara[†,1,2], K. Kinoshita[3], M. Kurata[1,2], M. Iwasaki[3], T. Natsui[1,2],
Y. Okayasu[1,2], I. Satake[1], M. Satoh[1,2], K. Uemura[3], Di Wang[1,2]
[1]High Energy Accelerator Research Organization (KEK), Tsukuba, Japan
[2]The Graduate University for Advanced Studies, SOKENDAI, Hayama, Japan
[3]Osaka Metropolitan University, Osaka, Japan

Abstract

The KEK e^-/e^+ LINAC supplies electron beams to SuperKEKB HER, PF and PF-AR, and positron beams to SuperKEKB LER. In addition to conventional manual tuning based on beam physics and operational experience, we also employ machine learning for beam tuning. In this paper, we report on beam diagnostics, data acquisition and analysis, and beam tuning using machine learning.

Beam tuning using machine learning has proven to be highly effective for increasing positron beam charge and reducing beam emittance. The parameters for these tunings are determined based on beam physics and operational experience, enabling efficient and rapid adjustments. However, it is not always possible to determine the optimal parameters. In beam tuning using machine learning, the choice of parameters to be optimized is critically important. While it is possible to infer key parameters that contribute to beam tuning and beam stability from beam physics models, it is not straightforward to examine all accelerator parameters or to evaluate the magnitude of their influence. Furthermore, identifying the factors that compromise beam stability remains a significant challenge.

To address this issue, we are attempting to analyze the data using explainable AI (XAI) techniques in order to extract the most important parameters affecting the beam. In this paper, we report an example of extracting beam-tuning parameters from large datasets.

KEK E-/E+ LINAC

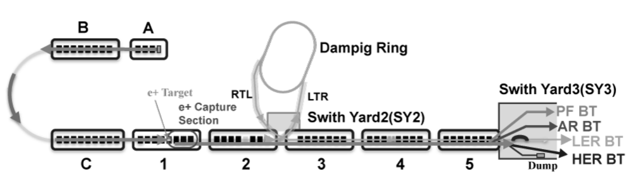

Figure 1: Layout of the KEK e-/e+ LINAC.

The KEK e^-/e^+ LINAC (the LINAC) serves as the common injector for four accelerators, with beam modes prepared according to the receiving accelerator. The beam repetition rate is 50 Hz, and the allocation of beam modes is adjusted in response to requests from the downstream accelerators. By utilizing the event timing system [1] for pulse-by-pulse control, the beam charge, energy, and optics are adjusted.

*Work supported by JSPS Grant-in-Aid for Transformative Research Areas A JP22H05113 and International Leading Research JP22K21347.
† fusashi.miyahara@kek.jp

Figure 1 shows a schematic layout of the LINAC. The LINAC is equipped with two electron guns (a thermionic gun and a photocathode RF gun [2]) and 226 accelerating structures, with 61 klystrons used to supply RF to these components. The beam energy is adjusted according to the target accelerator; for HER injection the beam is accelerated up to 7 GeV. At the klystron and SLED (pulse compressor) outputs and at the entrances of the accelerating structures, the phase and amplitude of the forward (input) and reflected RF are measured by RF monitors [3]; in total, 65 RF monitors are installed across the injector.

In the LINAC, a total of about 450 DC quadrupole magnets, DC steering magnets, and bending magnets are installed. Since the beam energy varies depending on the beam mode, 46 pulsed quadrupole magnets, 73 pulsed steering magnets [4], and 4 pulsed bending magnets for beam switching are also installed to provide the optimal optics for each mode.

The LINAC is equipped with approximately 100 stripline-type beam position monitors (BPMs), which can be read out with a resolution better than 7 mm [5], and all BPM data are synchronized with the beam. In addition, about 20 high-precision beam profile monitors capable of beam-synchronized measurements [6] and about 60 older monitors for visual inspection are installed. Furthermore, a synchrotron radiation monitor is installed in the J-ARC, enabling non-destructive measurement of the energy spread.

DATA ARCHIVING SYSTEM

Almost all the equipment in the injector is controlled via EPICS [7]. Data archiving is carried out in two ways: (1) raw data saved for every beam shot, and (2) sampled data stored through the ArchiverAppliance [8] either periodically or when device settings are changed.

The shot-by-shot data consist of BPMs, RF monitors, and pulsed magnets, with raw data saved in text format by each EPICS IOC. These data are synchronized with the beam because, since both the event codes corresponding to the beam modes distributed through the event timing system and the shot IDs assigned to each beam shot are simultaneously recorded. These data are synchronized with the beam, as they are simultaneously recorded with the event codes corresponding to the beam mode distributed via the event timing system and the shot IDs assigned to each beam shot. Such data can be extracted as beam-synchronized datasets for any monitor, beam mode, and specified time. Since there are about 2000 parameters in the synchronized data, outputting long-term (several days or

ISBN: 978-3-95450-262-2 ISSN: 2673-5350 doi: 10.18429/JACoW-IBIC2025-TUBC02

more) synchronized data from the raw files requires considerable time. This makes it unsuitable for long-term data analysis with machine learning. To address this, the data are converted into a Pandas Dataframe [9] and stored in table-format HDF5 [10]. In machine learning, it is not always necessary to use all parameters. In some cases, only the parameters considered essential are extracted, either to avoid using strongly correlated parameters or to prevent issues such as overfitting. Using HDF5 in table format allows immediate extraction of only the specified parameters, reducing memory usage.

The ArchiverAppliance collects not only beam position and charge but also data from nearly all devices in the accelerator, ranging from vacuum levels to temperatures at various locations. Since the data collected by the ArchiverAppliance can be easily visualized by anyone through a web-based UI, it is extremely useful for accelerator operation. Abnormal device behaviours, parameter oscillations on the order of minutes, and long-term drifts over several months can all be checked quickly. It is also possible to examine correlations between multiple parameters by studying their temporal variations. However, most of these data are asynchronous with the beam, meaning that correlations hidden within beam jitter, such as beam position fluctuations, cannot be identified. Moreover, since the data are stored on a channel-by-channel basis rather than on an event-by-event basis, it is necessary to extract beam-synchronized data when investigating correlations with the beam. When many parameters are to be included in the analysis, creating a dataset for analysis can take a considerable amount of time.

BEAM TUNING WITH ML

At the LINAC, Bayesian optimization is applied to various beam tuning tasks, all of which have proven to be highly effective. Beam tuning in accelerators is particularly well-suited to Bayesian optimization because the parameters required for tuning can be reasonably estimated based on beam physics and prior manual tuning experience, and the initial values provided are usually close to the optimum. Although Bayesian optimization can encounter issues such as the exploration–exploitation trade-off and instability of Gaussian process models in noisy environments, we describe several examples of its successful application in the LINAC.

The positron beam injected into the SuperKEKB LER is produced by irradiating a tungsten target with a 2.9 GeV electron beam, and then captured and accelerated in a strong solenoidal magnetic field [11]. Since the positron yield depends on the irradiation position and profile of the beam, the steering magnets and quadrupole magnets upstream of the target are adjusted so that the captured bunch charge is maximized [12]. When using Bayesian optimization, this tuning is completed within about ten minutes. The positron beam is accelerated up to 1.1 GeV and injected into the damping ring (DR) [13] to reduce its emittance. The electron beams injected into the target (the 1st and 2nd bunches) are generated by a thermionic gun, then bunched through two sub-harmonic bunchers, a pre-buncher, and a buncher, and subsequently accelerated to 58 MeV by two accelerating structures before being merged into the main beamline via a vertical pulsed bending magnet. When the initial conditions of the electron beam change, a drift occurs in the vertical (y-direction) orbit after merging, which can reduce the beam transmission to the target and consequently lower the charge of the generated positron beam. To address this, when the average positron bunch charge falls below a threshold, vertical orbit correction is automatically performed. Figure 2 shows how the charge is maintained by automatic tuning.

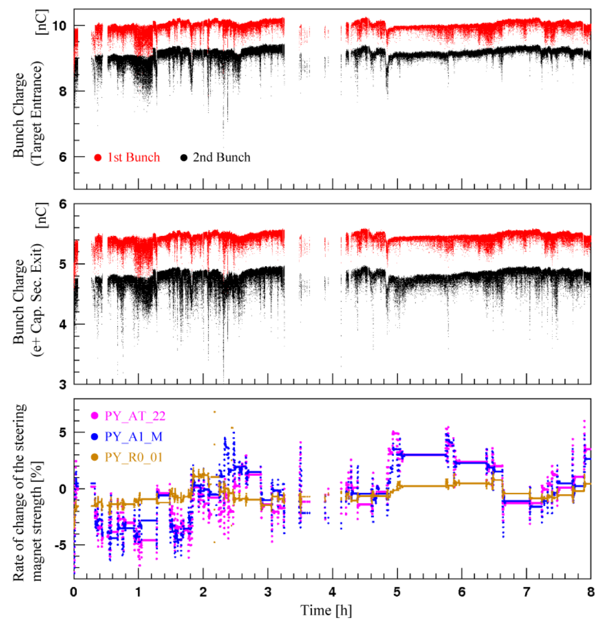

Figure 2: Example of automatic tuning with Bayesian optimization, showing maintained charge of the electron beam incident on the target and the generated positron beam. PY_AT_22 and PY_A1_M are pulsed magnets installed upstream and downstream of the vertical pulsed bending magnet, respectively, while PY_R0_01 is installed at the entrance of the J-ARC.

Since the beam quality upstream of the DR does not affect the beam quality downstream of the DR, and only a small amount of adjustment is required to restore the yield lost due to such drifts, these tunings are performed even during injection into the LER.

At the exit of the positron capture section, both the energy spread and the beam size are large. Therefore, in the straight section up to the branching line toward the DR, 104 quadrupole magnets and 51 steering magnets are installed at short intervals. Including the entire beam transport line up to the DR, there are about 200 parameters in total. It is difficult to accurately predict the longitudinal and transverse phase-space distribution of the positron beam at the capture section exit through simulation, making it impossible to determine the optimal optics purely by calculation. Thus, the magnet strengths downstream of the capture section were divided into several tuning segments, and Bayesian optimization was applied sequentially from upstream

ISBN: 978-3-95450-262-2 ISSN: 2673-5350 doi: 10.18429/JACoW-IBIC2025-TUBC02

so as to maximize the beam transmission efficiency. As a result of this tuning, for a 9 nC electron beam incident on the target, the charge measured just before the DR injection line improved from 3.3 nC to 4.0 nC [12].

Since low emittance beams are required for injection into the SuperKEKB HER/LER [14], suppressing emittance growth within the LINAC is an important issue. In the LINAC, emittance growth is largely caused by kicks from wakefields when the beam passes off-center through the accelerating structures. Although the BPM centers are calibrated to coincide with the magnetic centers of the quadrupole magnets, offsets relative to the centers of the accelerating structures cannot be measured with the beam, and each component is subject to alignment errors. In addition, the longitudinal and transverse phase-space distributions of the beam are also important, but these are extremely difficult to measure. Therefore, the beam orbit that suppresses emittance growth due to wakefields in the accelerating structures must be determined experimentally.

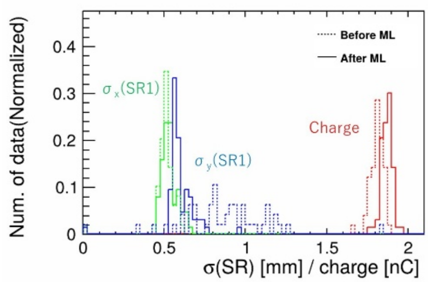

Figure 3: Beam size and charge before and after tuning with machine learning. The dashed line indicates the values before tuning, and the solid line indicates those after tuning.

Emittance growth caused by deviations of the beam from the optimal orbit leads to an increase in beam size. To address this, Bayesian optimization is used to determine the orbit that minimizes the beam size measured by the synchrotron radiation (SR) monitor installed in the SuperKEKB HER beam transport line (BT). In this tuning, the way the beam passes through the hole in the target—namely, the orbit correction from the J-ARC to the target—proved to be effective. This is consistent with the adjustments made by experienced operators when minimizing emittance through manual tuning. After optimization, the beam size is observed to be reduced (Fig. 3). Table 1 summarizes the normalized emittances before and after the correction, showing that minimizing the beam size also reduces the emittance. Since the SR monitor allows non-invasive beam measurements, it is extremely useful. At a beam repetition rate of 5 Hz, this tuning can also be completed in about 10 minutes.

Table 1: Comparison of emittance at HER BT before and after tuning with Bayesian optimization

	$\varepsilon_{n,x}$ [μm]	$\varepsilon_{n,y}$ [μm]
Before tuning	64.9±8.6	45.6±11.0
After tuning	29.2±5.1	46.9±13.0

BIG DATA ANALYSIS

Physics-based correlation analysis

In accelerators, many parameters are expected to be physically correlated, and it is important to experimentally verify such correlations. At the LINAC, analyses can be performed by combining large sets of synchronized data with data collected by the ArchiverAppliance. In the previous section, it was shown that emittance growth can be suppressed by adjusting the beam orbit. Injection efficiency into the HER is also thought to be correlated with the beam orbit; however, it is not obvious which orbit locations in the injector are the most critical.

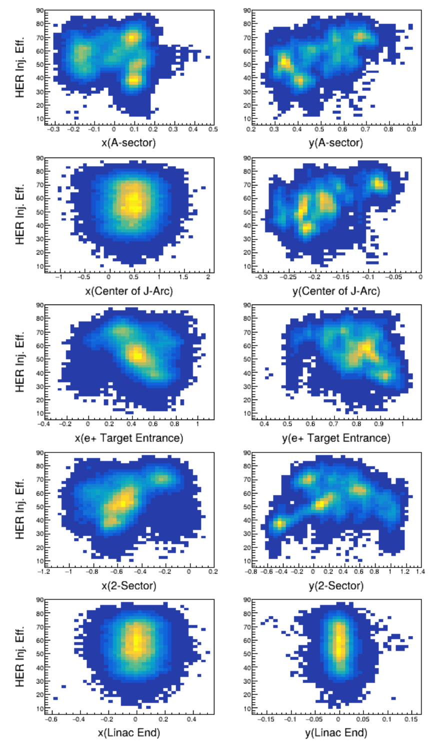

Figure 4: Correlation between the electron beam position and the injection efficiency into the HER. The upper panels correspond to an upstream section of the LINAC, while the lower panels show the BPM located just before the positron target.

To investigate this, correlations between beam positions measured by BPMs in the injector and the injection efficiency were studied using five days of data. When parameters are physically correlated, clear correlations can often be observed by analyzing several days of data, but analyzing longer-term data may obscure them owing to the interplay of complex factors. In practice, the analysis of data over periods of several months or longer requires the use of machine learning. Injection efficiency was obtained from the ArchiverAppliance, which is not linked to the event system; synchronization was therefore performed by comparing timestamps. Figure 4 shows the correlation between beam position and injection efficiency at five locations in order from upstream in the LINAC. Except for the LINAC end, correlation structures with injection efficiency can be seen at all positions; however, at locations other than

ISBN: 978-3-95450-262-2 ISSN: 2673-5350 doi: 10.18429/JACoW-IBIC2025-TUBC02

the BPM at the target entrance, the correlation structures are divided into several island-like patterns. This is considered to arise from indirect correlations, since those locations are optically connected to the regions that directly affect injection efficiency. In contrast, a clear correlation is observed at the entrance of the target. This BPM is located upstream of the positron target, where the electron beam passes through a hole in the target. Since the optics downstream of the positron target are optimized to maximize positron transmission, the β-function for the HER electron beam becomes large in this region. Consequently, orbit variations are also larger, and the impact of wakefields in the accelerating structures is expected to be more significant here than in other regions. It was also confirmed that the beam angle at the target position exhibits a clear correlation with the injection efficiency. This result is also consistent with the experimental findings in the previous section, where emittance growth was suppressed by orbit correction from the J-ARC to the target. At the LINAC end, no correlation is observed, because from the 3-sector onward orbit feedback is active, keeping the orbit constantly adjusted to the same trajectory.

Data analysis based on the physical background is useful for identifying the parameters required for beam tuning, and the LINAC provides an environment that enables detailed analyses.

Analysis using Explainable AI

Although parameters critical to beam tuning and beam instabilities in accelerators can be to some extent predicted based on physical considerations, there exist many parameters that simultaneously influence the beam, which imposes limitations on correlation analysis. Moreover, correlation analysis has difficulty capturing nonlinear relationships. To address this, we have begun efforts to evaluate beam-tuning–relevant parameters using XAI, cally SHAP. SHAP (SHapley Additive exPlanations) is a method that quantifies the contribution of each feature to a prediction made by a trained model, using Shapley values from cooperative game theory [15]. This approach allows visualization of the influence of individual features on a single prediction, as well as aggregated evaluation of global feature importance across the model. Because SHAP inherently explains situations where all features contribute simultaneously, it is expected to be a useful tool for accelerator operation and beam physics studies. However, caution must be exercised since SHAP serves as a tool for model explainability, but it does not provide any guarantee of causality. For example, in the case described in the previous section—identifying beam orbits associated with deteriorated injection efficiency—beam positions measured at multiple BPMs exhibit multicollinearity, and directly applying such injection data into SHAP fails to provide meaningful results.

Here, we present an example of analyzing correlations between RF and beam performance. At the LINAC, an Axion-like Particle (ALP) search experiment [16] is being considered during periods without injection into downstream rings, using the beam dump line. In this experiment, it is important to reduce beam losses upstream of the detector in order to lower the background in the physics data. Due to the high beam energy, even small losses in the beam duct can generate a large number of secondary particles, so beam halo-induced losses are also a significant concern. To investigate the parameters contributing to background, we analysed about two months of post-tuning data with TensorFlow [17] and SHAP. The inputs consisted of 672 RF parameters (RF amplitude and phase measured at the klystron, SLED, and the entrance of the accelerating structure), 837 magnet current settings, and 661 environmental temperatures. The outputs were beam transmission from the upstream LINAC to just before the beam dump, and signals from optical-fiber beam-loss monitors installed along the dump line.

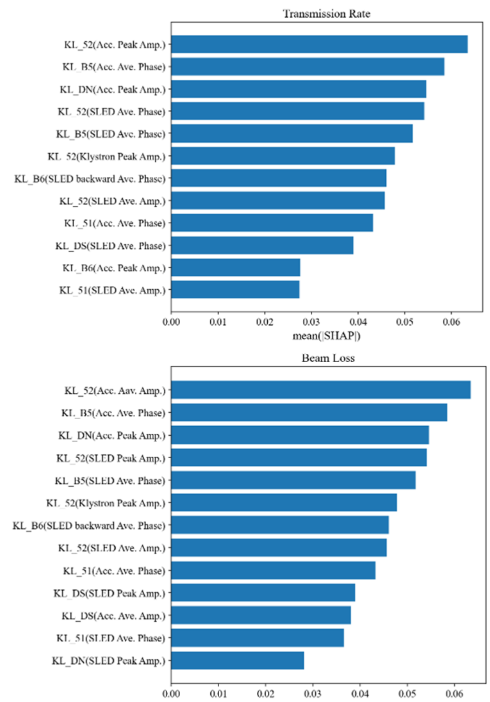

Figure 5: The upper panel shows the importance of RF parameters with respect to the beam transmission, while the lower panel shows their importance for the beam loss, expressed as the absolute SHAP values.

Figure 5 shows parameters identified as important for beam transmission and beam loss. All high-importance parameters were RF-related, with the strongest influence from the upstream B-sector (KL_B*) and the downstream 5-sector (KL_5*). The RF in the B-sector primarily affects the energy spread at the entrance of the J-Arc. Since collimators are installed in the J-Arc, the part of the energy distribution that is collimated depends on the beam orbit (energy) and energy spread. From the 5-sector to the dump, several bending magnets are located, making the 5-sector RF important for transporting the energy-spread beam to the dump with minimal loss.

From the SHAP analysis, it was predicted that increasing the phase of KL_B5 by about +1.5° from its operational setting would reduce the beam transmission by ~1% but substantially decrease beam loss. We therefore measured

ISBN: 978-3-95450-262-2 ISSN: 2673-5350 doi: 10.18429/JACoW-IBIC2025-TUBC02

the relationship between the KL_B5 phase, beam loss, and transmission (Fig. 6). The blue dashed line indicates the operational setting, while at +1.5° (red dashed line) the transmission decreases by about 1%, but beam losses are reduced nearly to the pedestal level. It is considered that the phase change of KL_B5 increased beam loss in the J-ARC, causing the energy tail that had been lost in the dump line to be collimated by the J-ARC collimators, which in turn contributed significantly to the overall reduction of losses.

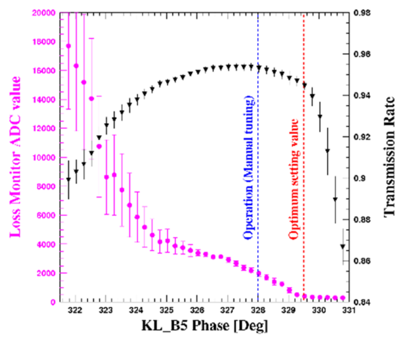

Figure 6: Beam loss as a function of klystron phase and beam transmission efficiency up to the beam dump.

In the LINAC, two klystrons are typically operated as a pair in order to equalize the acceleration of the head and tail of the bunch, with their phases set symmetrically around the crest phase. Therefore, the SHAP-based indication of adjusting the phase of a single klystron was highly meaningful. Nevertheless, there remain issues to be addressed in SHAP analyses. For example, in Fig. 5, klystron KL_DN is listed as an important parameter; however, the beam does not pass through the accelerating structure powered by KL_DN, which is used for energy compression in the DR injection line. This is in fact an irrelevant parameter and should have been excluded, but it likely represents a spurious correlation—possibly with Low Level RF acting as a latent variable.

Going forward, we plan to continue advancing research aimed at improving and stabilizing beam quality through the use of SHAP, other XAI techniques, and their combination with deep learning.

CONCLUSION

The KEK e^-/e^+ LINAC supplies beams to four circular accelerators, providing beam conditions tailored to the requirements of each. We reported on the overview of the injector, the monitoring system, and data archiving. Since the LINAC involves many parameters and beam conditions that require tuning, Bayesian optimization has been actively adopted for beam adjustment, and it has been successfully applied to tasks such as maximizing and maintaining positron beam charge and reducing electron beam emittance. In addition, big data analysis is used to evaluate the parameters necessary for optimization. More recently, explainable AI (XAI) with SHAP has been introduced to extract parameters effective for tuning and to estimate those contributing to beam stability. As an example, we presented the use of SHAP to identify RF parameters important for reducing beam losses.

REFERENCES

[1] H. Kaji *et al.*, “Construction and Commissioning of Event Timing System at SuperKEK”, in *Proc. IPAC’14,* Dresden, Germany, Jun. 2014, pp. 1829-1832. doi:10.18429/JACoW-IPAC2014-TUPRI109

[2] T. Natsui *et al.*, “Injector Linac Upgrade and New RF Gun Development for SuperKEKB”, in *Proc. eeFACT2016*, Daresbury, UK, Oct. 2016, pp. 74-78. doi:10.18429/JACoW-eeFACT2016-TUT2H2

[3] H. Katagiri *et al.*, “RF Monitor System for SuperKEKB Injector Linac”, in Proc. IPAC’18, Vancouver, Canada, April 2018, pp. 2128-2130. doi:10.18429/JACoW-IPAC2018-WEPAK016

[4] Y. Enomoto *et al.*, “A New Pulsed Magnet Control System in the KEK Electron Positron LINAC”, in *Proc. IPAC’18,* Vancouver, Canada, April 2018, pp. 2121-2123. doi: 10.18429/JACoW-IPAC2018-WEPAK014

[5] R. Ichimiya, K. Furukawa, F. Miyahara, M. Satoh, and T. Suwada, “High Position Resolution and High Dynamic Range Stripline Beam Position Monitor (BPM) Readout System for the KEKB Injector Linac Towards the SuperKEKB”, in *Proc. IBIC'14*, Monterey, CA, USA, Sep. 2014, paper WEPD04, pp. 637-641.

[6] M. Satoh *et al.*, “Synchronized Beam Position Measurement for SuperKEKB Injector Linac”, in *Proc. IPAC'18*, Vancouver, Canada, Apr.-May 2018, pp. 4159-4162. doi:10.18429/JACoW-IPAC2018-THPMF045

[7] EPICS, https://epics-controls.org/

[8] Archiver Appliance, https://epicsarchiver.readthedocs.io/en/latest/

[9] W. McKinney, “Data Structures for Statistical Computing in Python”, in *Proc. The 9th Python in Science Conference,* Dresden, Germany, June 2010, pp. 51-56.

[10] HDF5, https://www.hdfgroup.org/solutions/hdf5/

[11] T. Kamitani *et al.*, “SuperKEKB Positron Source Construction Status”, in *Proc. IPAC’25*, Taipei, Taiwan, Jun. 2025, pp. 1651-1655. doi:10.18429/JACoW-IPAC2025-WEXN1

[12] T. Natsui *et al.*, “Upgrade of KEK electron/positron injector LINAC using pulsed magnets and machine learning”, in *Proc. IPAC’14,* Dresden, Germany, Jun. 2014, pp. 579-581. doi:10.18429/JACoW-IPAC2014-MOPRI004

[13] M. Kikuchi *et al.*, “Design of Positron Damping Ring for Super-KEKB”, in *Proc. IPAC'10*, Kyoto, Japan, May 2010, paper TUPEB054, pp. 1641-1643.

[14] K. Akai *et al.* “SuperKEKB collider”, *Nucl. Instrum. Methods Phys. Res. A*, vol. 907, pp. 188-199, 2018. doi:10.1016/j.nima.2018.08.017

[15] S. M. Lundberg and Su-In Lee, “A Unified Approach to Interpreting Model Predictions”, in *Proc. NIPS* 2017, Long Beach, USA, Dec. 2017.

[16] A. Ishikawa, Y. Sakaki and Y. Takubo, “Search for axion-like particles with electron and positron beams at the KEK linac”, *Prog. Theor. Exp. Phys.*, vol 2022, Issue 11, p. 113B05, 2022. doi:10.1093/ptep/ptac129

[17] TensorFlow, https://www.tensorflow.org